4. AN INVESTIGATION OF CURVED CRACK PROPAGATION

by

Hans Bergkvist† and Lan Guex††
Institut CERAC SA, CH-1024 Ecublens,
Switzerland

Abstract

So far the analysis of cracks propagating along a non-straight path has been almost exclusively restricted to the onset of crack propagation under mixed mode loading conditions and to incipient crack branching.

In the present paper the main interest is focussed on the propagation phase. Different directional criteria are investigated from a theoretical point of view. As an illustration a configuration loaded so that a curved crack path is obtained is analyzed numerically using finite element methods.

Directional criteria are of two principally different types. One group consists of criteria in which the field around the original, the unbranched crack provides the information used. Such criteria are thus projective in nature. It is to be expected that, for the continuously extending crack, these criteria would at most apply to the initiation. For cases where a flaw is opened up outside of the main crack, a projective criterion might be strictly valid as long as the flaw does not significantly change the field around the main crack tip.

In a real propagation situation the field at the crack tip is constantly modified as the crack advances. In a criterion called a propagation criterion, the actual field around the extreme of a crack with a kinked tip should be used as input information.

In the paper the relative merits and shortcomings of five criteria are investigated. The whole analysis is limited to two-dimensional, isotropic and linearly elastic configurations and, unless otherwise indicated, plane strain conditions are assumed to prevail.

While currently used criteria for onset of crack propagation in a mixed mode loading situation give different predictions

---

† Senior Staff Scientist

†† Staff Scientist

for the angle of incipient branching, the present paper demonstrates that the trajectory of a curved crack to a large extent is independent of the choice among these criteria. The theoretical results have been verified by an analysis of the propagation phase through an incremental description using finite element calculations. A scheme using a path independent contour integral scheme permitting a separation of the stress intensity factors has proven a powerful tool for the analysis.

INTRODUCTION

In the past the main interest in the analysis of crack propagation along non-straight paths has been linked primarily with the onset under mixed mode conditions and with incipient crack branching [1-4]. Attempts to settle questions raised by conflicting theories, have resulted in a large number of papers [5-12].

Hussain et al [13] have calculated the stress field around the end of a crack with a kinked tip. By letting the length of the kink go to zero it was found that the stress field even in the limit does not coincide with the one for the unkinked crack. It is clear that, in a situation where the crack growth takes place as a continuous extension of a pre-existing crack, this result does invalidate results based on assumptions of stress field continuity, cf. Nuismer [14].

The consequences, however,are more far reaching. It means that not even the direction of incipient branching can be deduced by continuum-mechanical calculations using the field around the unbranched, the unkinked crack. In other words, a directional criterion has to be formulated, which means that an additional and independent assumption has to be brought into the picture, either separately or as an element of a generalized fracture criterion. Even in the latter case though, it is convenient to consider the directional criterion and the proper fracture criterion as separately imposed non-continuum-mechanical conditions.

Naturally a good directional criterion should reflect the physical processes that govern the material separation in the process region close to the crack tip. This also means that the directional criterion for onset of crack propagation and the one for the subsequent growth do not necessarily have to be the same, particularly so if the material separation processes are different in the two situations.

In the present paper the main interest is focussed on the propagation phase. Different directional criteria are investigated from a theoretical point of view. As an illustration a configuration loaded so that a curved crack path is obtained is analyzed numerically through an incremental description using finite element methods.

DIRECTIONAL CRITERIA

Directional criteria are of two principally different types. Some criteria are projective in nature, in the sense that the field around the original, the unbranched crack provides the information used. In view of what was pointed out in the introduction, it is to be expected that, for the continuously extending crack, these criteria would at most apply to the initiation. For cases where a flaw is opened up outside of the main crack, a projective criterion might be valid, at least approximatively, as long as the flaw does not significantly change the field around the main crack tip.

In a real propagation situation the field at the crack tip is constantly modified as the crack advances. In criteria called propagation criteria the actual field around the extreme of a crack with a kinked tip has to be used as input information.

In the subsequent sections the relative merits and shortcomings of five commonly used criteria listed below are investigated.

PROJECTIVE CRITERIA

A: Propagation perpendicularly to the direction of the maximum principal stress [1]

B: Propagation in the direction of minimum strain energy density [2]

C: Propagation in the direction of maximum strain energy release rate [3]

PROPAGATION CRITERIA

D: Propagation in pure opening mode, mode I [4]

E: Propagation so that the local stress field is symmetric with respect to the branch plane [15]

The whole analysis is limited to two-dimensional, isotropic and linearly elastic configurations, and, unless otherwise indicated, plane strain conditions are assumed to prevail.

A: PRINCIPAL STRESS CRITERION

For a general in plane loading situation the near-tip stress field will be determined by the stress intensity factors K_I and K_{II}, for the opening and sliding mode respectively. In fact

$$\tau_{r\theta} = \frac{\cos \theta/2}{2\sqrt{2\pi r}} \left[K_I \sin \theta + K_{II}(3 \cos \theta - 1) \right] \tag{1}$$

with respect to a polar coordinate system r, θ with its origin at the crack tip and $\theta = \pm\pi$ corresponding to the crack faces. The angle θ_o for which $\tau_{r\theta} = 0$ will determine the orientation of the principal axis and it will thus be given from the relation

$$K_I \sin \theta_o + K_{II}(3 \cos \theta_o - 1) = 0 \tag{2}$$

as has been indicated in [1].

Denoting the ratio K_{II}/K_I by λ, the solution of (2) is simplified to

$$\theta_o^* \simeq -2\lambda \tag{3}$$

for small λ.

B: STRAIN ENERGY DENSITY CRITERION

In numerous publications Sih has advocated the idea that the local strain energy density, S, at a certain distance r_o from the crack tip should be the governing quantity for the fracture process, cf. [2,11,12]. More specifically, a flaw would form in a direction θ_o for which the strain energy density has a minimum, once it has reached a certain critical value, and this flaw would then join the main crack.

Under general in plane loading conditions, S takes the following form

$$S = a_{11} K_I^2 + 2a_{12} K_I K_{II} + a_{22} K_{II}^2 \tag{4}$$

where the coefficients a_{ij} are given in [2].

The angle θ_o is given from the relation $\partial S/\partial\theta = 0$ which can be reduced to

$$\cos 2\theta_o [(1-3\lambda^2)\tan 2\theta_o + 4\lambda] - (\varkappa - 1)\cos \theta_o [(1-\lambda^2)\tan \theta_o + 2\lambda] = 0 \tag{5}$$

where again λ is used to denote the ratio K_{II}/K_I. In order to verify that the solution to (5) does correspond to a minimum, one has to check that the additional condition $\partial^2 S/\partial\theta^2 > 0$ is fulfilled.

Generally speaking and in contrast to other theories θ_o will depend on Poisson's ratio ν through κ which is $3-4\nu$ under plane strain and $(3-\nu)/(1+\nu)$ under plane stress conditions. However, the conditions for the two expressions within brackets to go to zero are

$$\left.\begin{aligned} \tan 2\theta_o &= -\frac{4\lambda}{1-3\lambda^2} \\ \text{and} \\ \tan \theta_o &= -\frac{2\lambda}{1-\lambda^2} \end{aligned}\right\} \qquad (6)$$

It is clear that these will be fulfilled simultaneously when λ is small, giving

$$\theta_o^* \simeq -2\lambda \qquad (7)$$

independently of ν, for $\nu > 0$.

C: STRAIN ENERGY RELEASE RATE CRITERION

The strain energy release rate for a virtual displacement of the crack tip in the θ-direction can be expressed in terms of a generalized J-integral quantity, which, cf. [3], can be written

$$J_\theta = \frac{\kappa+1}{8\mu}\left[(K_I^2+K_{II}^2)\cos\theta - 2K_IK_{II}\sin\theta\right] \qquad (8)$$

where the meaning of κ is the same as for criterion B and where μ is the shear modulus. This criterion says that the crack will grow in such a direction θ_o for which J_θ has a maximum. The solution of the equation $\partial J/\partial\theta = 0$ is

$$\tan\theta_o = -\frac{2\lambda}{1+\lambda^2} \qquad (9)$$

which for small values of $\lambda = K_{II}/K_I$ reduces to

$$\theta_o^* \simeq -2\lambda \qquad (10)$$

D: PURE MODE CRITERION

Several authors, among those Kalthoff [4] and Bilby [16] have proposed the condition of pure mode propagation $K_{II} = 0$, $J_2 = 0$ as a directional criterion. The main physical argument in favour of this idea is that material separation in the process region should take place in pure opening mode.

E: LOCAL SYMMETRY CRITERION

Pärletun [15] has stressed the numerical difficulties in calculating J_2 by means of a path independent integral and pointed out that instead of actually calculating K_{II} or J_2 and determining the direction for which these quantities are zero, one might equally well study the conditions for

local stress field symmetry with respect to the crack increment plane. Local stress field symmetry is at hand when the stress field component parallel to the crack increment σ_x is the same in two points, situated symmetrically with respect to the branch plane, and located sufficiently close to the crack tip to make the singularity terms dominant in the stress field.

COMPUTATIONAL ASPECTS

Except maybe for very special cases, an analytical solution of the curved crack problem seems to lie far beyond what can be hoped to be obtained. A logical alternative is thus to use an incremental description of the crack growth, studied by means of finite element methods. Recently Stern et al [17] have proposed a method using a path independent contour integral scheme by which a separation of the stress intensity factors K_I and K_{II} can be obtained. In fact, as shown in Appendix I, closed form expressions for K_I and K_{II} can be extracted from [17].

By using 8-node isoparametric elements and a 2 x 2 Gaussian integration, by letting the integration path go through the integration points and embrace typically 20 elements out of a total of around 150, we have found the stress intensity factors to be stable to within 1% for K_I and 2% for K_{II} when $K_{II}/K_I > 10\%$ for changes in the mesh near the crack tip. This larger integration loop gives improved results in comparison with [18] where a close tip integration path was used. The results from a test case

with a slanted edge crack in a rectangular plate has been found to correspond to within 1% with values obtained from boundary collocation.

ILLUSTRATIVE EXAMPLE

The above criteria have been applied to the configuration shown in Fig. 1. Some 150 8-node isoparametric elements were used to model the plate. Fig. 2 shows a typical mesh once the crack has grown to some extent. The near-tip elements were rectangular 8-node quarterpoint ones, Fig. 3, except for cases where a more accurate description of the near field might be needed, as when applying the local symmetry criterion. In this case triangular quarterpoint elements that describe the singularity correctly also in the interior of the element have been used [19,20], Fig. 4.

RESULTS

The crack trajectories according to the different criteria have been determined using an incremental description. The increment Δx has been held fixed, typically equal to 0.066a, 2a being the total width of the plate.

In the projective criteria, K_I and K_{II} have been determined using the integral scheme (AI:8). The values obtained have then been used to predict the orientation of

the next crack increment as given by the different criteria A, B and C.

When applying the propagation criteria, a crack extension equal to half the increment length has been made in four different directions within $\pm 10^{o}$ from the orientation of the previous increment. Then the direction for which $K_{II} = 0$, criterion D, or local symmetry is at hand, criterion E, can be deduced by linear interpolation. Then the increment has been extended in this direction. In this way the criteria are fulfilled in a position corresponding to the midpoint of the increment.

The results are summarized in Fig. 5. As can be seen, the difference between the curves is hardly distinguishable on the scale of the figure. Furthermore, as shown in Fig. 6, the differences in trajectories for increment sizes equal to half of and twice the original one are negligible.

Kitagawa et al [21] have pointed out that if the path taken by the crack deviates from the correct one for some reason, the effects of K_{II} will tend to compensate for the deviation. This implies that a step by step investigation of crack growth should give stable results. One would thus expect that the effect of an angular deviation in an early stage of the propagation would be annihilated after a number of crack increments. Fig. 7 supports this idea showing that the latter part of the trajectories where the first step is oriented at 0 and -45^{o} to the horizontal do coincide.

Cotterell [22-24] has used the concept of class I and class II cracks in a series of papers on crack path stability and these ideas have lately been further explored by Leevers et al [25]. In essence a pre-existing crack in a mixed mode field would be class II, since it never returns to its original orientation, whereas the smooth curved crack propagation would be an example of a class I crack, since it exhibits a tendency to go back to its original path after being subjected to a perturbation.

When it comes to the influence of Poisson's ratio on the predicted crack paths, a recent paper by Bilby [26] based on earlier works,[27] and [16],provides some material for quantitative conclusions. Consider Fig. 8. A semi-infinite crack is subjected to a mixed mode loading situation giving rise to the stress intensity factors K_I and K_{II}. Assuming a kink of length unity to be present and denoting the stress intensity factors at the end of the kink by k_1 and k_2, then the functions h_i relating the two sets of stress intensity factors

$$\left.\begin{aligned} k_1 &= h_1(\theta)K_I + h_2(\theta)K_{II} \\ k_2 &= h_3(\theta)K_I + h_4(\theta)K_{II} \end{aligned}\right\} \qquad (11)$$

are given on graphical form in [26].

Using, as in previous sections, λ to designate the

ratio K_{II}/K_I and analogously λ^* for k_2/k_1 the graph in Fig. 8 can be established.

An immediate observation is that the curves representing the predictions from criterion B for different values of Poisson's ratio ν all fall close together and in a region where $|\lambda^*/\lambda|$ attains small values. Furthermore the influence of Poisson's ratio is only noticeable for large values of $|\lambda|$, which is in agreement with what was said on criterion B above. One would thus expect the trajectories predicted by criterion B for materials with different Poisson's ratio to differ somewhat in a starting phase where $|\lambda|$ is large. After a few increments, a short propagation distance, however, the different curves would tend to join. Furthermore, since $|\lambda|$ is decreasing, the radius of curvature would increase. These effects are illustrated in Fig. 9 where as expected the low Poisson's ratio curve shows the slowest convergence.

Ingraffea [28] has used different criteria for a crack trajectory study and found a large discrepancy between them. In view of the present analysis, it seems highly unlikely that these differences should be due to the influence of Poisson's ratio.

DISCUSSION

A number of currently used directional criteria, such

that are projective in nature as well as true propagation criteria have been investigated. For a smooth crack path, i.e. a crack path having a continuously turning tangent, $\theta_o^* = 0$ in the criteria A, B and C. Through the equations (3), (7) and (10) this condition implies $\lambda = 0$, i.e. $K_{II} = 0$ which is the main feature of the criteria D and E.

In this incremental description, however, the crack path is composed of a sequence of straight segments. Since the values of the stress intensity factors for a certain crack tip position do depend on the orientation of the crack tip, the fact that, generally speaking, $\lambda \neq 0$ and thus $\theta_o^* \neq 0$ does consequently not mean any contradiction.

As can be seen from Fig. 5, the differences in the predicted trajectories are vanishingly small. It could thus be argued that, as long as the question of how the material separation in the process region close to the crack tip takes place has not been answered satisfactorily, the choice of directional criterion becomes more a matter of computational ease.

In this context the integration scheme allowing a separation of the stress intensity factors becomes a particularly powerful tool. In fact the only restrictions imposed on the applicability of the expression (AI:8) are that the crack faces are straight and free of traction inside the integration loop, a requirement that is easily met in an incremental crack growth description. When on the other hand

the symmetry criterion is applied, care has to be taken to assure that the points observed fall within a region where the singularity is determining the stress field and thus the influence from higher order terms is negligible.

In cases where the main interest is linked with the trajectory on the whole, as for example in different aspects of fragmentation, the detailed behaviour at onset has a small influence. In addition the often claimed importance of Poisson's ratio is shown to be almost non-existent. Ironically enough these matters so far have retained the most extensive attention in the analysis of mixed mode fracture problems.

REFERENCES

1. F. Erdogan and G.C. Sih, Journal of Basic Engineering, 85 (1963) 519-527.
2. G.C. Sih, International Journal of Fracture, 10 (1974) 305-321.
3. H.C. Strifors, International Journal of Solids and Structures, 10 (1974) 1389-1404.
4. J.F. Kalthoff, in Dynamic Crack Propagation, Noordhoff International Publishing, Leyden (1973) 449-458.
5. H. Anderson, Journal of the Mechanics and Physics of Solids, 17 (1969) 405-417.
6. K. Palaniswamy and W.G. Knauss, International Journal of Fracture Mechanics, 8(1972) 114-117.
7. J.G. Williams and P.D. Ewing, International Journal of Fracture Mechanics, 8(1972) 441-446.
8. I. Finnie and A. Saith, International Journal of Fracture, 9(1973) 484-486.
9. P.D. Ewing and J.G. Williams, Internaional Journal of Fracture, 10 (1974) 135.
10. I. Finnie and H.D. Weiss, International Journal of Fracture, 10 (1974) 136-138.
11. G.C. Sih and M.E. Kipp, International Journal of Fracture, 10 (1974) 261-265.
12. G.C. Sih, International Journal of Fracture, 10 (1974) 279-283.
13. M.A. Hussain, S.L. Pu and J. Underwood, Proceedings of the 1973 National Symposium on Fracture Mechanics, Part II, ASTM STP 560, 2-28.
14. R.J. Nuismer, International Journal of Fracture, 11 (1975), 245-250.
15. L.G. Pärletun, Determination of the growth of branched cracks by numerical methods, Report LUTMDN/(TMHL - 3005)/ 1-51/(1976), Lund Institute of Technology, Lund (1976).

16. B.A. Bilby, in The Mechanics and Physics of Fracture, Churchill College, Cambridge (1975) 1-10.

17. M. Stern, E.B. Becker and R.S. Dunham, International Journal of Fracture, 12 (1976) 359-368.

18. H. Bergkvist and L. Guex, in Numerical Methods in Fracture Mechanics, Swansea (1978) 810-813.

19. R.S. Barsoum, International Journal for Numerical Methods in Engineering, 10 (1976) 25-37.

20. R.S. Barsoum, International Journal for Numerical Methods in Engineering, 11 (1977) 85-98.

21. H. Kitagawa, R. Yuuki and T. Ohira, Engineering Fracture Mechanics, 7 (1975) 515-529.

22. B. Cotterell, International Journal of Fracture Mechanics, 1 (1965) 96-103.

23. B. Cotterell, International Journal of Fracture Mechanics, 2 (1966) 526-533.

24. B. Cotterell, International Journal of Fracture Mechanics, 6 (1970) 189-192.

25. P.S. Leevers, J.C. Radon and L.E. Culver, Journal of the Mechanics and Physics of Solids, 24 (1976) 381-395.

26. B.A. Bilby, G.E. Cardew and I.C. Howard in Fracture 1977, Waterloo, Canada, 3 (1977) 19-24.

27. B.A. Bilby and G.E. Cardew, International Journal of Fracture, 11 (1975) 708-712.

28. A.R. Ingraffea, in Numerical Methods in Fracture Mechanics, Swansea (1978) 235-248.

APPENDIX I

SEPARATION OF K_I AND K_{II} BY MEANS OF A PATH INDEPENDENT INTEGRAL

Betti's reciprocal work theorem in the case of vanishing body forces can be written as

$$\int_{\Gamma} (u\hat{t}-\hat{u}t)ds = 0 \qquad \text{(AI:1)}$$

where Γ is the boundary of a simply connected and bounded region. u and t and $\hat{u}$ and $\hat{t}$ denote the displacement and traction vectors respectively corresponding to two solutions of a particular equilibrium problem.

Equation (AI:1) can be written

$$I = -\int_{\Gamma'} (u\hat{t}-\hat{u}t)ds = \int_{\Gamma''=\Gamma-\Gamma'} (u\hat{t}-\hat{u}t)ds \qquad \text{(AI:2)}$$

where Γ' is a circle embracing the crack tip. Orienting a polar coordinate system as in Fig. AI:1 the first integral in (AI:2) can be expressed as

$$I = \int_{-\pi}^{\pi} \left[\hat{\sigma}_r u_r + \hat{\sigma}_{r\theta} u_\theta - \sigma_r \hat{u}_r - \sigma_{r\theta}\hat{u}_\theta\right] r_o d\theta \qquad \text{(AI:3)}$$

Here

$$u_r = r^{\frac{1}{2}}\left[f_1(\theta)K_I + f_2(\theta)K_{II}\right] + o(r^{\frac{1}{2}})$$

and

$$\sigma_r = r^{-\frac{1}{2}}\left[g_1(\theta)K_I + g_2(\theta)K_{II}\right] + o(r^{-\frac{1}{2}})$$

(AI:4)

and analogously for the other components. f_i and g_i are the well-known functions that describe the angular form of the near-tip fields.

The corresponding expressions for the auxiliary problem have the forms

$$\hat{u}_r = r^{-\frac{1}{2}}\left[\hat{f}_1(\theta)C_1 + \hat{f}_2(\theta)C_2\right] \qquad (AI:5)$$

$$\hat{\sigma}_r = r^{-3/2}\left[\hat{g}_1(\theta)C_1 + \hat{g}_2(\theta)C_2\right] \qquad (AI:6)$$

The functions $\hat{f}_i$ and $\hat{g}_j$ are given in [17]. In the expression given therein for $\hat{\sigma}_{r\theta}$, however, a factor 3 seems to be missing in the cos 3θ/2-term.

Carrying out the integration one finds

$$I = C_1K_I - C_2K_{II}. \qquad (AI:7)$$

Since $\hat{u}$ and $\hat{t}$ are linear combinations of C_1 and C_2 it is clear that the second integral in (AI:2) will be a linear combination of C_1 and C_2. The evaluation of this integral

will thus permit the calculation of K_I and K_{II}. In fact, rearranging the terms in the integrand one finds

$$\begin{aligned}
K_I = \int_{\Gamma''} \Big\{ & u_r\left[(7\cos\tfrac{3\theta}{2} - 3\cos\tfrac{\theta}{2})n_1 + 3(\sin\tfrac{3\theta}{2} + \sin\tfrac{\theta}{2})n_2\right] A_1 \\
& + u_\theta\left[3(\sin\tfrac{3\theta}{2} + \sin\tfrac{\theta}{2})n_1 + (\cos\tfrac{3\theta}{2} + 3\cos\tfrac{\theta}{2})n_2\right] A_1 \\
& - (\sigma_r n_1 + \sigma_{r\theta} n_2)\left[(2\kappa + 1)\cos\tfrac{3\theta}{2} - 3\cos\tfrac{\theta}{2}\right] A_2 \\
& + (\sigma_{r\theta} n_1 + \sigma_\theta n_2)\left[-(2\kappa - 1)\sin\tfrac{3\theta}{2} + 3\sin\tfrac{\theta}{2}\right] A_2 \Big\} \, ds \\
K_{II} = -\int_{\Gamma''} \Big\{ & u_r\left[(7\sin\tfrac{3\theta}{2} - \sin\tfrac{\theta}{2})n_1 - (3\cos\tfrac{3\theta}{2} + \cos\tfrac{\theta}{2})n_2\right] A_1 \\
& + u_\theta\left[-(3\cos\tfrac{3\theta}{2} + \cos\tfrac{\theta}{2})n_1 + (\sin\tfrac{3\theta}{2} + \sin\tfrac{\theta}{2})n_2\right] A_1 \\
& + (\sigma_r n_1 + \sigma_{r\theta} n_2)\left[(2\kappa + 1)\sin\tfrac{3\theta}{2} - \sin\tfrac{\theta}{2}\right] A_2 \\
& - (\sigma_{r\theta} n_1 + \sigma_\theta n_2)\left[(2\kappa - 1)\cos\tfrac{3\theta}{2} - \cos\tfrac{\theta}{2}\right] A_2 \Big\} \, ds
\end{aligned} \qquad (AI:8)$$

with:

$$A_1 = -\frac{\mu}{2(1+\kappa)\,(2\pi r^3)^{\frac{1}{2}}}$$

$$A_2 = \frac{1}{2(1+\kappa)\,(2\pi r)^{\frac{1}{2}}}$$

where μ and $\varkappa$ are defined in criterion B and n_1, n_2 are the components of the outwards unit normal to Γ''.

For the case where the crack faces are unloaded and straight within the integration path, there will be no contributions from these segments. So, the integration is limited to the outer part of the integration loop on which the stresses and displacements can be calculated by finite element methods.

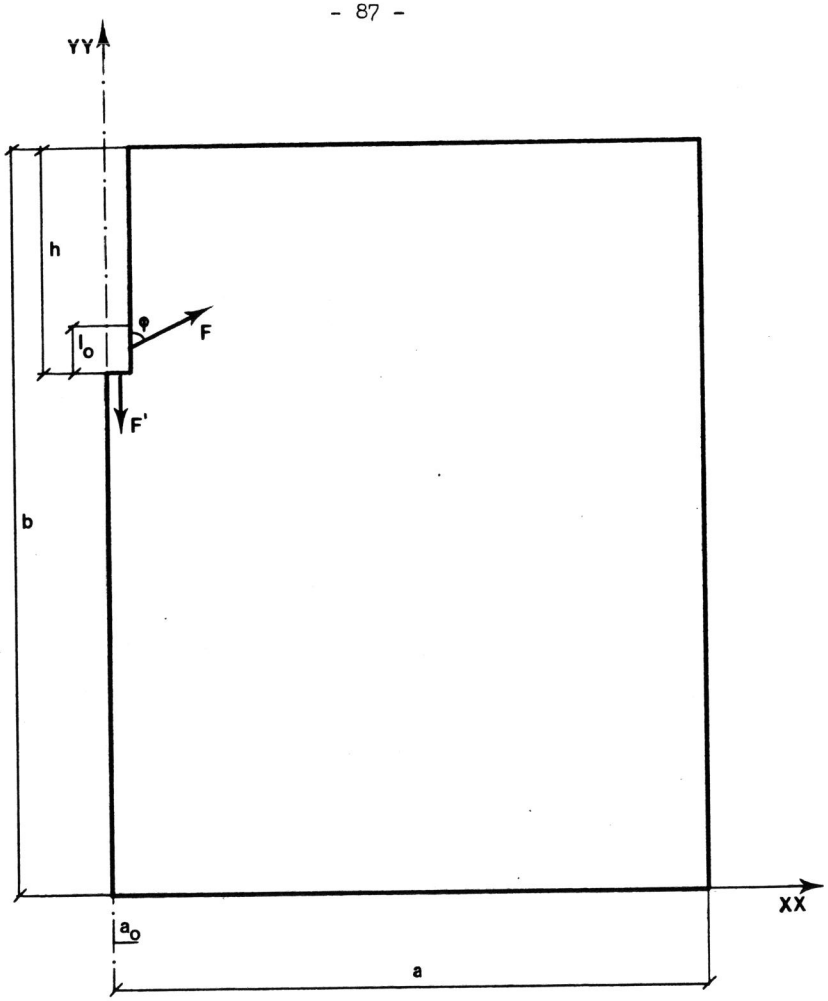

Fig. 1 The plate configuration analysed (only the right half shown). The forces F' and F are in equilibrium.
a = 0.70 m, b = 0.86 m, a_o = 0.0285 m, h = 0.26 m, l_o = 0.05 m, φ = 63.5 degrees.

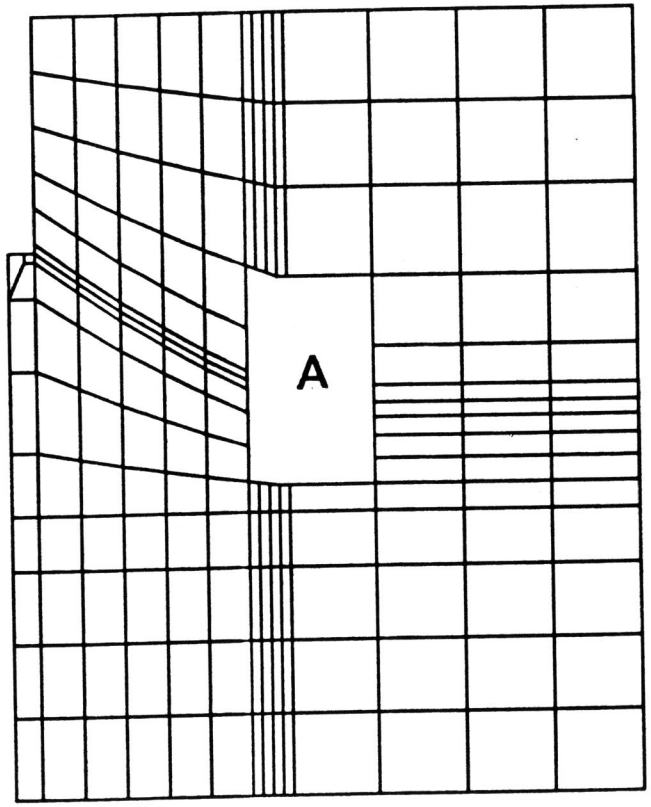

Fig. 2 Typical mesh structure. The near-tip region A is enlarged in Figs. 3 and 4.

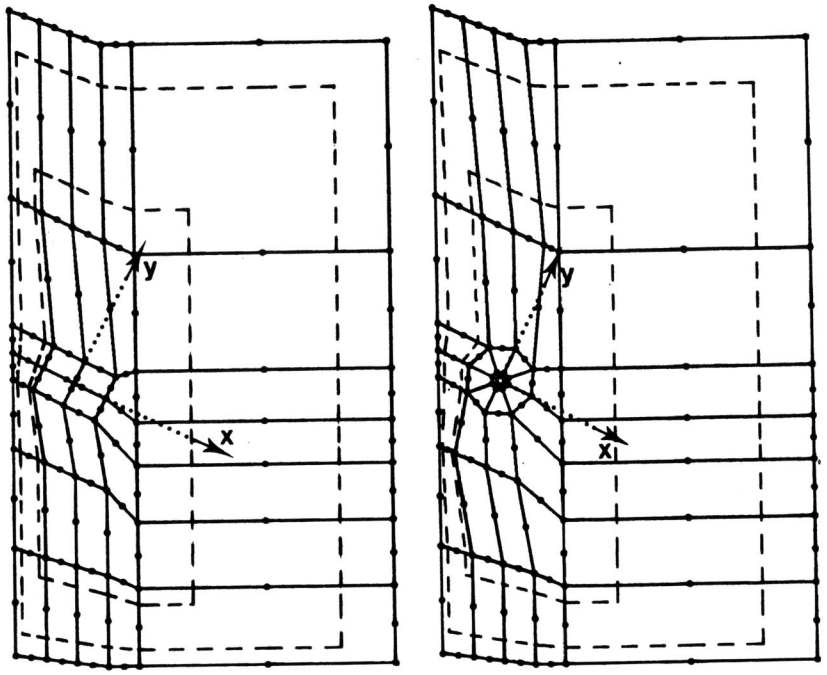

Fig. 3 The near-tip mesh with four rectangualar quarter-point 8-node isoparametric elements surrounding the tip itself. The position of the crack tip corresponds to the origin of the local coordinate system x-y.
The dashed lines indicate two integration paths.

Fig. 4 The crack tip surrounded by eight degenerated quarterpoint elements.

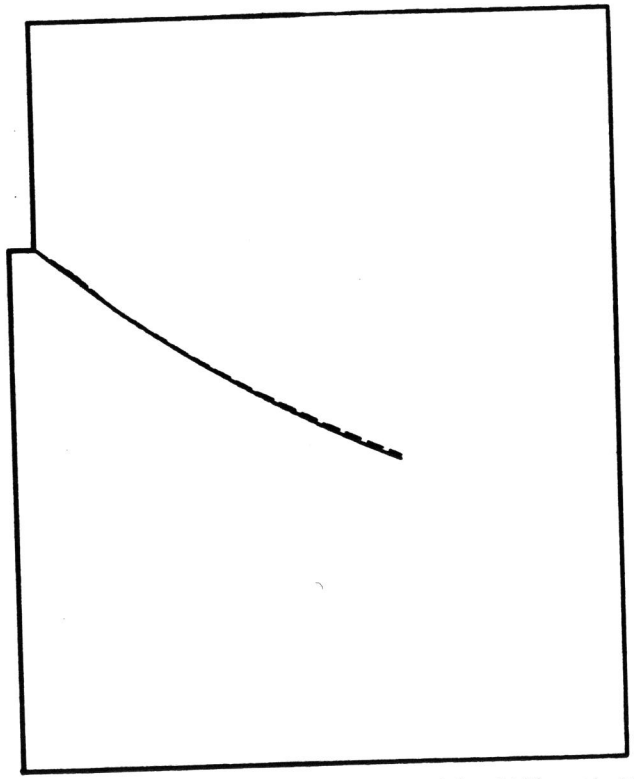

Fig. 5 Crack trajectories predicted by different criteria. Projective: solid and dotted lines, propagation criteria: dashed line.

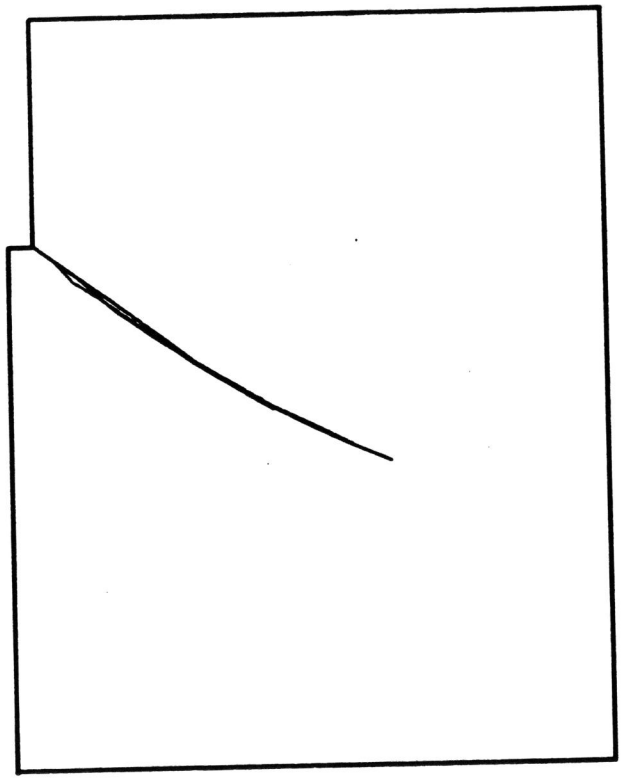

Fig. 6 Trajectories for crack increments $\Delta x = 0.132a$, $0.066a$ and $0.033a$. Total plate width $2a$. Criterion B, Poisson's ratio $\nu = 0.25$.

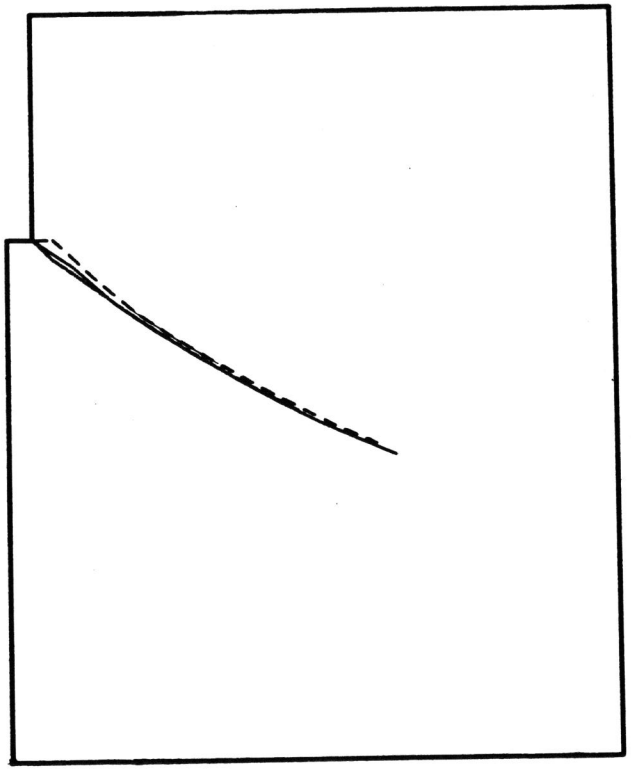

Fig. 7 Influence on the trajectory from an initial angular deviation. $\theta_1 = 0^o$(upper), $\theta_1 = 45^o$ (lower). The solid curve in the middle is the trajectory for criterion B, Poisson's ratio $\nu = 0.25$.

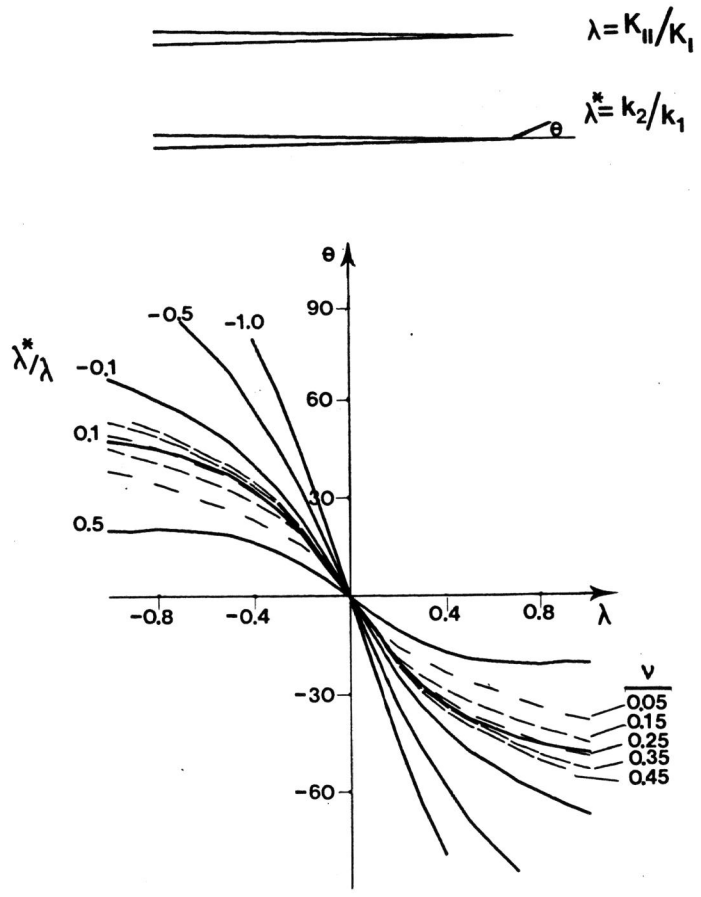

Fig. 8 The kink angle θ versus the ratio $\lambda = K_{II}/K_I$ for different ratios λ^*/λ where $\lambda^* = k_2/k_1$. The dashed lines give the predictions as given by criterion B for Poisson's ratio $\nu = 0.05$ (0.10)0.45.

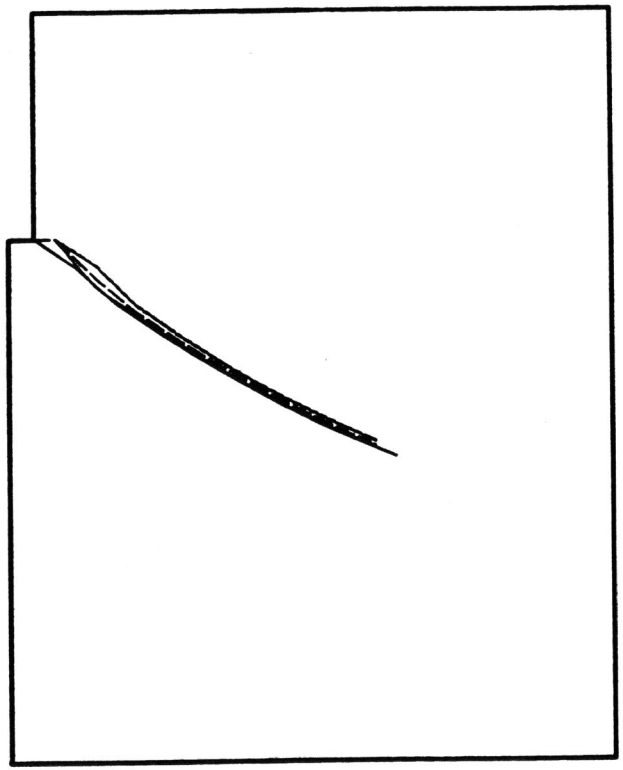

Fig. 9 The influence on the trajectory in criterion B from Poisson's number ν given an initial angular deviation. Upper curve $\nu = 0.05$, middle curve $\nu = 0.25$, lower curve $\nu = 0.45$. The solid line from the corner of the slot is the prediction from criterion B and $\nu = 0.25$.

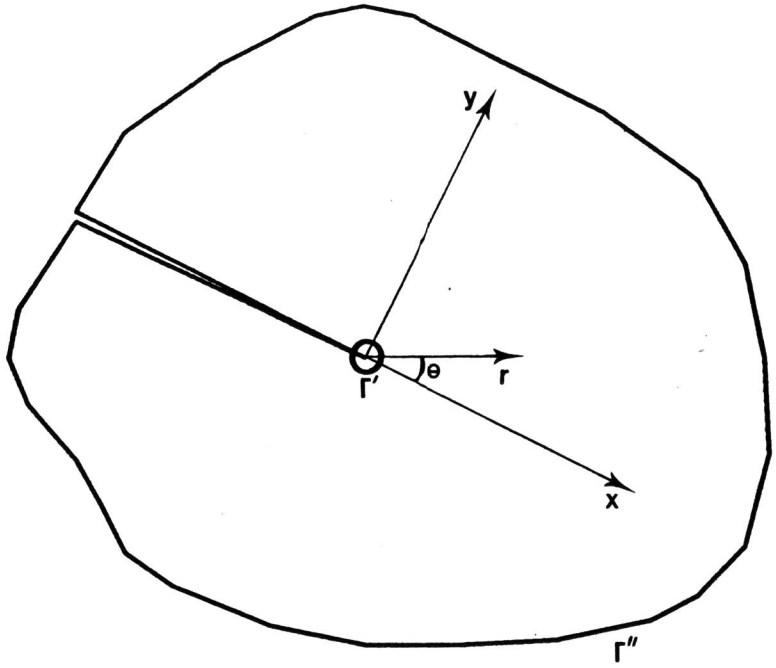

Fig. AI:1 The boundary $\Gamma = \Gamma' + \Gamma''$, where Γ' is a small circle of radius r_o embracing the crack tip.